Modeling of Extinction in Turbulent Diffusion Flames by the Velocity-Dissipation-Composition PDF Method

A. T. NORRIS*
Institute for Computational Mechanics in Propulsion, NASA Lewis Research Center, 22800 Cedar Point Road, Brookpark, OH 44142

S. B. POPE
Sibley School of Mechanical and Aerospace Engineering, Cornell University, Ithaca, NY 14853

The velocity-dissipation-composition probability density function (pdf) method is used to model a turbulent $CO/H_2/N_2$–air-piloted jet diffusion flame in the regime of extinction. The thermochemistry is modeled by a three-scalar simplified formulation obtained by the intrinsic low-dimensional manifold (ILDM) method. Calculations are performed for five different jet velocities, and the scalar pdfs are compared with experimental data. Overall good agreement is obtained between the calculations and the experimental results, with the only significant difference being the high level of scatter in the experimental data compared with the pdf results: reasons for this difference are discussed. The pdf method is found to predict flame extinction at approximately the same jet velocity as that of the experiment. A small amount of local extinction is observed in the pdf results for the high-jet-velocity cases.

INTRODUCTION

One of the attractions of using probability density function (pdf) methods to model turbulent combustion is that the reaction term can be treated exactly [1, 2]. This feature provides a method of modeling reacting flows where strong turbulent/chemical interactions occur. One feature of such flows that is of interest for many engineering applications is the phenomenon of extinction.

In this paper, the transport equation for the joint pdf of velocity, dissipation and composition is solved for the case of a piloted turbulent, $CO/H_2/N_2$–air diffusion flame investigated by Masri et al. [3]. The chemical reaction is modeled by a three-scalar scheme, created by the intrinsic low-dimensional manifold (ILDM) method of Maas and Pope [4, 5]. Five different flow conditions of increasing jet velocity are calculated, corresponding to the case of fully burned flame through to extinguished flow. The numerical and experimental pdfs of the species are then compared, and the performance of the pdf model discussed.

EXPERIMENT

The experiment flow chosen for this study is the $CO/H_2/N_2$–air flame of Masri et al. [3]. In this experiment, composition data are obtained for different flame conditions, varying from fully burned to extinguished.

The apparatus consists of a central fuel jet with inside diameter $D_j = 7.2$ mm, surrounded by an annulus of 18.0 mm outside diameter, containing the pilot flame. This jet assembly is mounted at the center of the exit plane of a 305.0 × 305.0 mm wind tunnel, which produces a uniform, low turbulence intensity flow of air. The fuel composition is 45% CO, 15% H_2, and 40% N_2 by volume, and the pilot flame consists of a lit, premixed flow of fuel and air in stoichiometric proportions.

With the co-flow velocity held constant at 15.0 m/s and the unburnt bulk velocity of the pilot held at 1.0 m/s, the effect of varying the fuel jet velocity is investigated. Five bulk fuel jet velocities of 98.0, 131.0, 147.0, 155.0, and

* Corresponding author.

COMBUSTION AND FLAME 100: 211–220 (1995)

Published by Elsevier Science Inc.

0010-2180/95/$9.50
SSDI 0010-2180(94)00092-7

164.0 m/s are studied, with extinction of the flame determined to be at 167.0 m/s.

Data from the experiment consists of the joint pdfs of composition taken at a point 72.0 mm downstream of the jet exit plane, and approximately 6.5 mm out from the axis. These pdfs were obtained by the Rayleigh–Raman scattering technique.

PDF MODEL

The PDF scheme used in this study is based on the velocity-dissipation joint pdf model of Pope [6], but extended to include composition variables. In this section, only the differences between this model and the model of Pope are discussed.

Modeled Velocity and Dissipation Equations

As with the model of Pope [6], the velocity and the logarithm of the turbulent frequency ω are modeled as Langevin-type processes, where $\omega \equiv \epsilon/k$, ϵ is the turbulent dissipation rate, and k is the turbulent kinetic energy. The basis of these models is that DNS results [7] show the Lagrangian velocity and $\log(\omega)$ to be well approximated by a Gaussian process, with an exponential autocorrelation.

The only difference between the models used in this work, and those of Pope [6] is that the value of the constant $C_{\omega 1}$ in the ω equation has been changed. Pope [6] obtains a value of $C_{\omega 1} = 0.04$ based on the performance of the model in several planar flows. However it has been found [8] that while this value of $C_{\omega 1}$ provides good results for planar flows, setting $C_{\omega 1} = 0.08$ gives superior results for axisymmetric flows. A similar correction has also been used with success by Anand et al. [9].

Model for Scalar Mixing

A stochastic model for the mixing of a set of σ scalars is also needed, and the simple relaxation model of Dopazo [10] was adopted. This model gives the Lagrangian evolution of the αth scalar ϕ_α as

$$\frac{d\phi_\alpha^*}{dt} = -\frac{1}{2}C_\phi \tilde{\omega}\left(\phi_\alpha^* - \tilde{\phi}_\alpha\right) + S_\alpha(\underline{\phi}), \qquad (1)$$

where $S_\alpha(\phi)$ is the chemical source term, representing the change in the αth scalar by chemical reaction for the composition ϕ, a tilde denotes a density-weighted mean, and $C_\phi = 2.0$. The mean value of ω appears in this equation, rather than the instantaneous value, as the equation has to satisfy

$$\frac{d\langle\phi_\alpha\rangle}{dt} = 0, \qquad \frac{d\langle\phi_\alpha^2\rangle}{dt} = -C_\phi\langle\omega\rangle\langle\phi_\alpha^2\rangle \qquad (2)$$

for the case of the decay of a passive scalar in constant-density homogeneous, isotropic turbulence [11]. Also it has been found [8] that using the mean value of ω based on the turbulent particles gives better results in the intermittent regions of the flow, without affecting the performance in the fully turbulent regions.

The advantage of using this mixing model is that it is a continuous scheme [1], as opposed to stochastic models such as those based on particle interaction, like Curl's model [12], and thus there are no sudden jumps in composition. This feature can be important in reacting flows, as the jump in composition can produce unphysical cold mixing across a flame sheet [13].

The disadvantages of the model are that it is nonlocal in composition space [13], and it is known to perform poorly in predicting scalar decay in homogeneous isotropic turbulence. Rather than the shape of the scalar pdf relaxing to a gaussian distribution, the model preserves the shape of the initial pdf. However in nonhomogeneous flows, it has been shown that faulty models can still produce almost correct results, due to the influence of other processes on the scalar pdf [14, 15].

THERMOCHEMISTRY

The ILDM method of Maas and Pope [4, 5] was used to generate the thermochemical model used in this study. The ILDM method is a general procedure for simplifying chemical kinetics, based on a dynamical systems approach, requiring only the full chemical mechanism and the dimension, n_r of the resulting

reduced mechanism as input. Given these inputs, the ILDM scheme identifies the time scale of each reaction for all allowed compositions. By freezing the n_r slowest reactions and letting the rest relax to equilibrium, a low-dimensional attracting manifold is obtained. This manifold is then projected onto a set of n_r species, referred to as the controlling variables. The rate of change of these controlling variables is known at all points on the manifold, completing the creation of the reduced mechanism.

For the $CO/H_2/N_2$–air system used in this study, the full mechanism and details of the ILDM method are described by Maas and Pope [4]. A three-scalar mechanism was obtained from the full system, with the three representative scalars being the mixture fraction ξ, and the mass fractions of CO_2 and H_2O, denoted by Y_{CO_2} and Y_{H_2O}, respectively. The reduced mechanism is stored in the form of composition increments due to reaction for given time intervals and specified initial composition. An adaptive tabulation method is used to store these increment tables. It should be noted that as ξ is a conserved scalar, only the increments of Y_{CO_2} and Y_{H_2O} need be stored. A section of the reaction table for the stoichiometric mixture fraction is shown in Fig. 1, with the structure of the adaptive tabulation scheme superimposed.

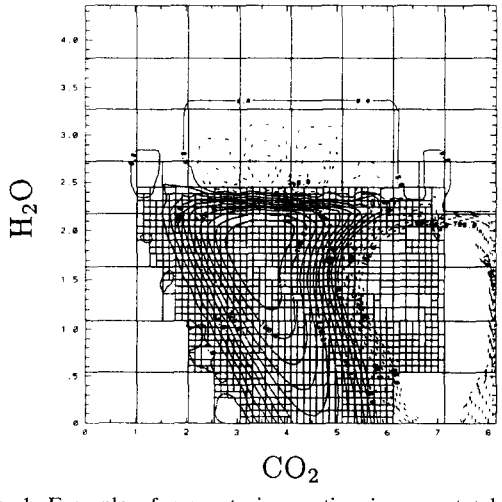

Fig. 1. Example of property in reaction increment table taken at $\xi = 0.375$. Property is the reaction rate of CO_2 in units of mol/kg.s $\times 10^{-3}$.

The level of accuracy with which the reduced mechanism represents the full chemical system depends on the number of controlling variables and the level of refinement of the look-up table. Both issues are discussed by Maas and Pope [16], who conclude that two controlling variables and a refinement level of 16 cells per axis provide a reasonable representation of the full chemical mechanism. The table used in this study has two controlling variables (plus mixture fraction), and has a higher refinement level of 64 cells per axis.

MONTE CARLO SOLVER

The solution of the pdf transport equation is obtained by a particle-based Monte Carlo scheme. By assuming that the flow is axisymmetric, almost parallel and statistically stationary, a two-dimensional parabolic solution scheme can be employed, which marches in the axial (x) direction. At each axial station, the density-weighted joint pdf $\tilde{f}$ is represented by a large number of fluid particles, with each particle having a radial position, (r), three velocity components, a value of frequency and a chemical composition. The number of fluid particles, N, is taken to be 40,000 to yield small statistical error, while still providing reasonable CPU times. The width of the solution domain expands to encompass the evolving radial profiles, and the length is restricted to 10 jet diameters from the jet exit. Profiles of mean quantities are obtained by the method of cross-validated least squares cubic splines [17].

INITIAL CONDITIONS

The initial conditions at the jet exit plane are the combination of three different flows, the jet, the pilot and the co-flow.

For the jet, the mass flow rate and the composition are known from the experiment. The initial velocity distribution is obtained by assuming a joint normal distribution, with the means and covariances of velocity corresponding to fully developed pipe flow, taken from Hinze [18]. The composition is taken to be uniform, and on dimensional grounds, ω is given by $\sqrt{k}/R_i$ (where R_i is the internal ra-

dius of the fuel jet) and log-normally distributed.

The mass flow rate and the preburned composition of the pilot are known from the experiment. By assuming the pilot to be fully burned at the jet exit, the mean composition, temperature and density are known. The low axial velocity of the pilot and the high temperature result in a Reynolds number of order 100, thus a uniform velocity is assumed, with all fluctuating quantities set to zero, as is the value of ω.

For the co-flow, the mean and fluctuating values of the axial velocity are known, and correspond to a turbulent boundary layer on the outside wall of the pilot jet. So as in the jet, the velocity distribution is assumed to be joint normal, with means and covariances obtained from experiment and supplemented by fully developed turbulent boundary layer data taken from Hinze [18]. On dimensional grounds, ω is taken as $\sqrt{k}/\delta_m$, where δ_m is the momentum thickness of the boundary layer.

Boundary conditions are an axis of symmetry for the center of the jet, and free stream conditions at the outer edge of the flow, corresponding to the known co-flow properties.

RESULTS

Five runs were performed for five different jet velocities, corresponding to the experimental conditions of Masri et al. [3]. The bulk jet velocities are 98.0, 131.0, 147.0, 155.0, and 164.0 m/s. In the experiments, extinction was found to occur at a bulk jet velocity of 167.0 m/s. Scatter plots of the composition were obtained for particles at $x/D_j = 10$ downstream and $1.8D_j$ out from the axis of symmetry, corresponding to the location where the experimen-

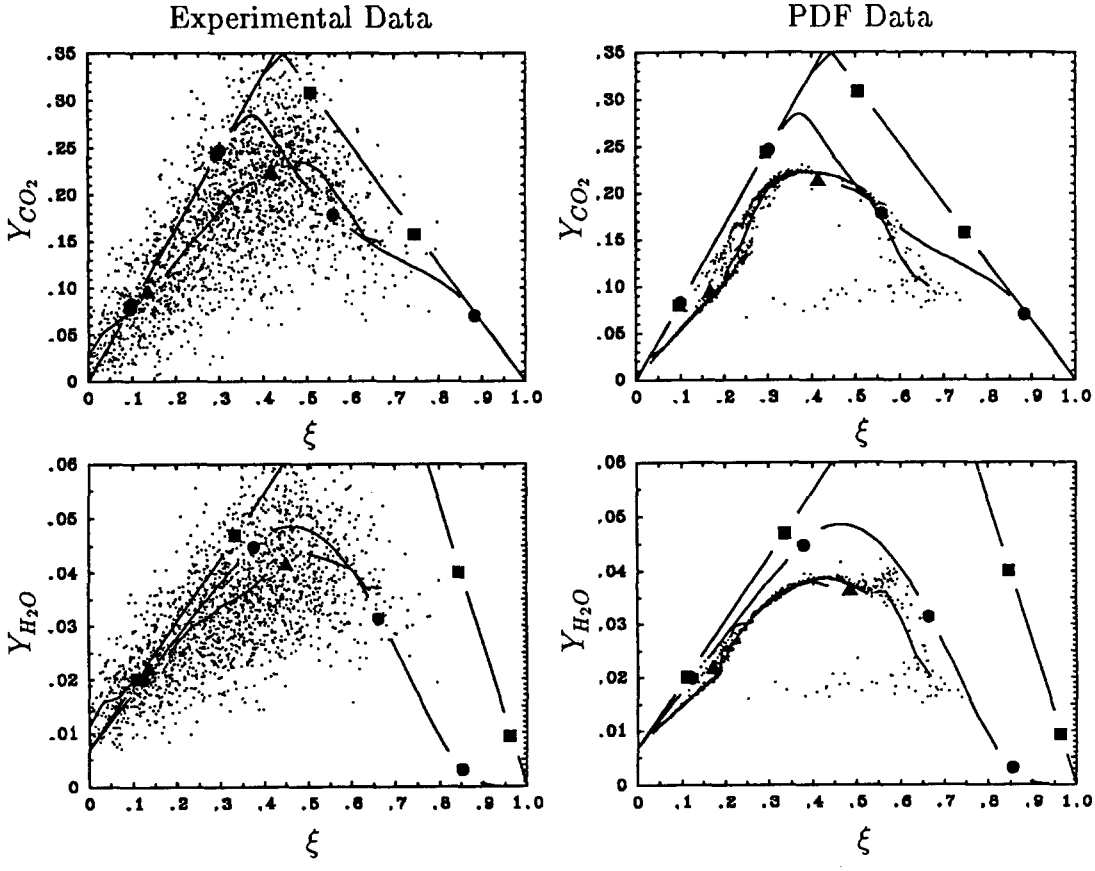

Fig. 2. Composition scatter plots for $CO/H_2/N_2$–air flame with jet velocity of 98 m/s. Experimental data in left column, pdf results in right column. –○–, equilibrium values; –□–, border of allowed region; –△–, conditional mean of data.

tal data were taken. These scatter plots for the five different runs are shown in Fig. 2–6, with the experimental data. Also plotted are the equilibrium limits for the $CO/H_2/N_2$–air reaction and the conditional averages of the experimental data, $\langle Y_{CO_2}|\xi\rangle$ and $\langle Y_{H_2O}|\xi\rangle$, where $\langle Y|\xi\rangle$ is the average of Y conditional on ξ. These equilibrium limits are calculated with the assumption of equal diffusivities and a Lewis number of one.

In comparing the experimental and calculated results, the most noticeable feature is that there is considerably greater scatter in the experimental data than in the numerical results. This difference can be attributed to three factors; experimental errors, differential diffusion, and deficiencies in the mixing model.

The experimental error is derived mainly from the chemiluminescence [19]. A mean correction can (and has been) applied to the data [3], but the statistical scatter still remains. Thus the mean of the data can be expected to be reasonably accurate, while the spread, or conditional variance, of the data may be less accurate.

The pdf model used in this study assumes that all species have equal diffusivities. However, this is known not be the case for real gas mixtures. In particular, the diffusivity of hydrogen is approximately four times that of nitrogen or oxygen. One effect of differential diffusion is that the definition of the mixture fraction becomes nonunique and so particles can appear outside the allowed region (defined with assumed equal diffusivity) and yet have realizable compositions. This effect is noticeable in the plots of experimental data in Figs. 2–6, where a small number of particles can be seen to lie outside the allowed region. Because the pdf model assumes equal diffusivities, no

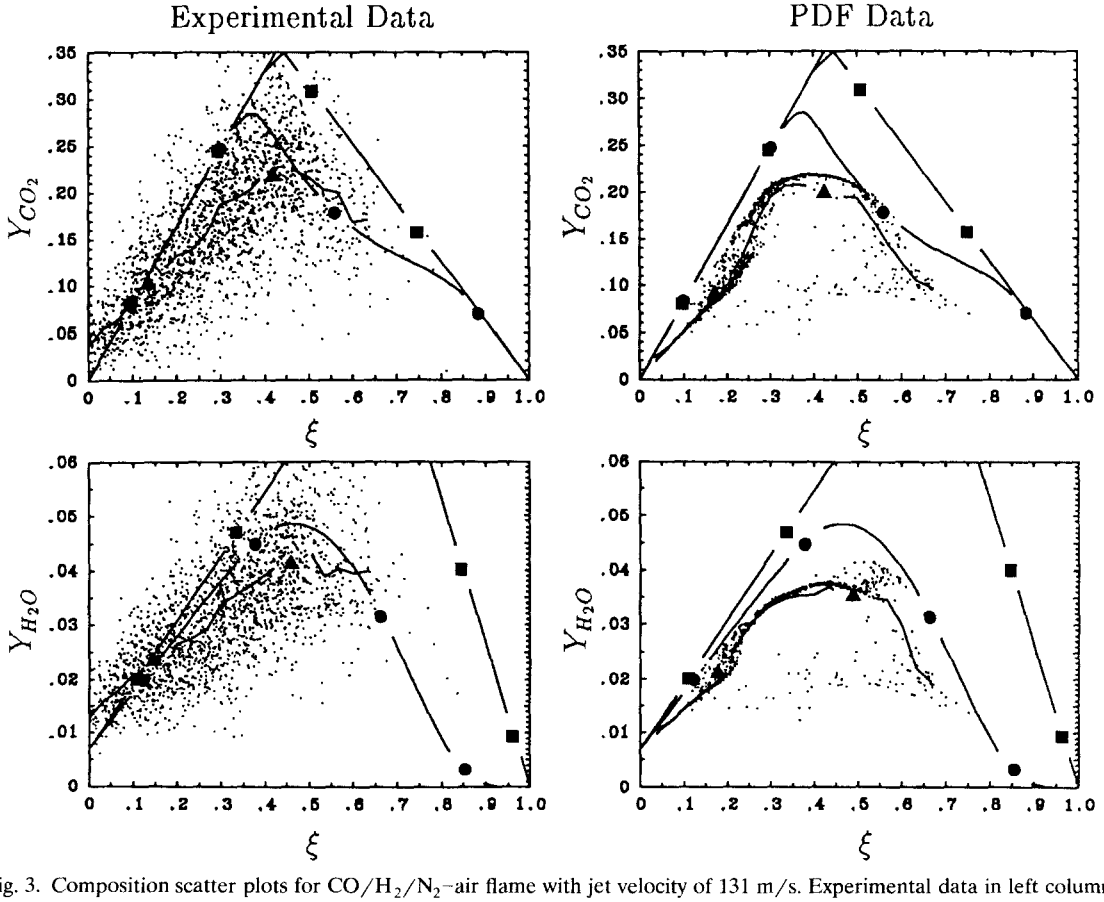

Fig. 3. Composition scatter plots for $CO/H_2/N_2$–air flame with jet velocity of 131 m/s. Experimental data in left column, pdf results in right column. –∅–, equilibrium values; –□–, border of allowed region; –△–, conditional mean of data.

particles can be found outside the allowed region in the pdf results.

The magnitude of the errors associated with experimental sources and the neglect of differential diffusion are illustrated by plotting the joint pdf of Y_{N_2} and ξ (Fig. 7). For the idealized case of no experimental error, equal diffusivities and inert N_2 (as assumed by the pdf model), the joint pdf would be represented by a straight line. However as Fig. 7 shows, this is not the case. The departure of the experimental data from the straight line has a standard deviation of approximately 10% of the mean value of Y_{N_2}. The conditional average $\langle Y_{N_2}|\xi\rangle$ though, is in reasonable agreement with the theoretical result. It is reasonable to assume that the other species will have at least this level of scatter, and hence the lower level of scatter in the pdf results is physically reasonable, and does not necessarily reflect some flaw in the model.

Having said this, the molecular mixing model does have known deficiencies that may affect the distribution of the particles in scalar space. The model is known to give an incorrect pdf in the decay of a scalar in homogeneous isotropic turbulence, and while the deficiencies are less pronounced in nonhomogeneous flows, it is probable that the model causes a degree of error in the distribution of particles in scalar space.

Despite the differences between the experimental data and the pdf results, some useful comparisons can be made. For the two lowest jet velocities (Fig. 2 and 3), the numerical results are in excellent agreement with the experimental conditional averages of Y_{CO_2} and Y_{H_2O}. Both the experimental and pdf results

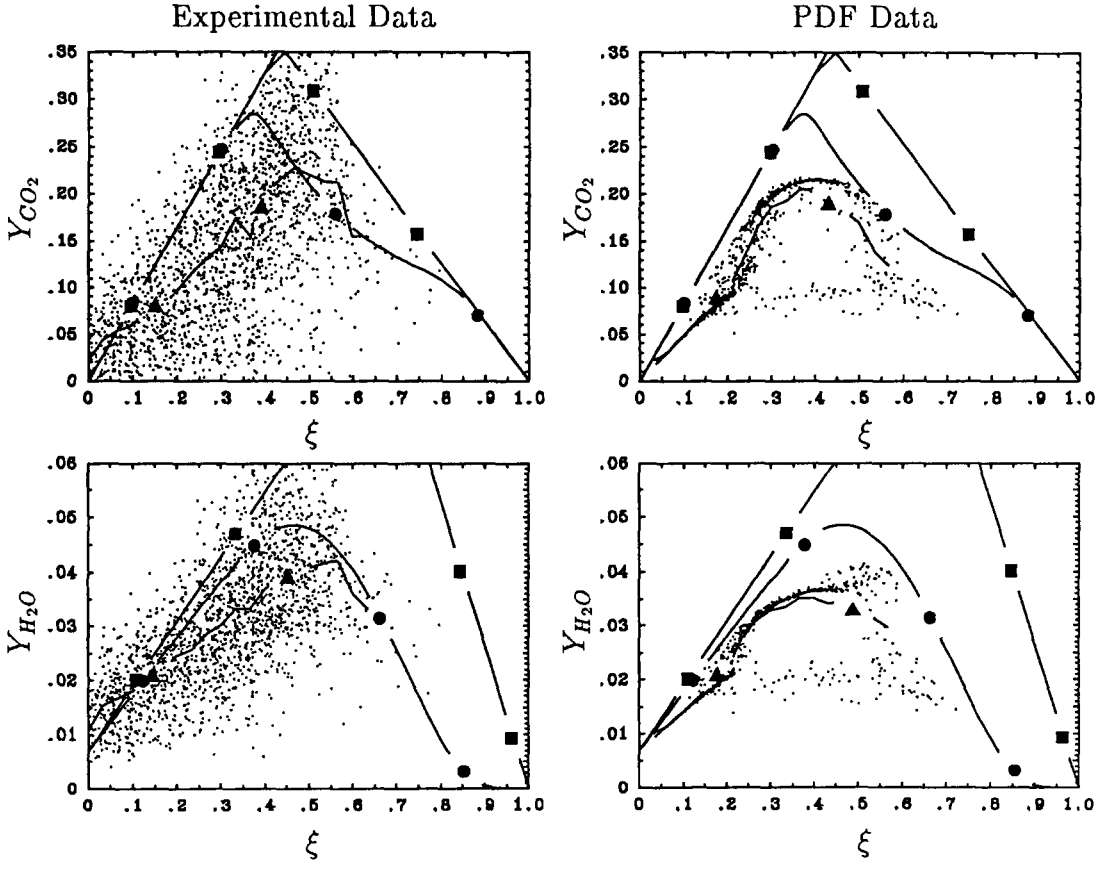

Fig. 4. Composition scatter plots for $CO/H_2/N_2$–air flame with jet velocity of 147 m/s. Experimental data in left column, pdf results in right column. –∅–, equilibrium values; –□–, border of allowed regions; –△–, conditional mean of data.

for these two flows show most of the points lying near the equilibrium line, but there are rare points corresponding to local extinction or incomplete combustion.

For the U_j = 147.0 m/s case (Fig. 4) the experimental data shows a similar form to that of the two lower velocity cases, but with the $\langle Y_{CO_2}|\xi\rangle$ profile falling further below the equilibrium line for lean compositions. Again the pdf results show good agreement with the conditional averages. The U_j = 155.0 m/s experimental data (Fig. 5) shows a further reduction of the value of $\langle Y_{CO_2}|\xi\rangle$ for lean compositions, and a corresponding drop in the $\langle Y_{H_2O}|\xi\rangle$ profile. The pdf results for this case show a bimodal form, with an approximately equal number of particles corresponding to unreacted and reacted compositions.

Finally, the U_j = 164.0 m/s case (Fig. 6) shows a mostly extinguished flame, with only a small level of reaction being sustained in the near-stoichiometric region of the composition. The pdf results agree reasonably well with the experimental data, with the majority of the particles being nonreactive.

For the three highest jet velocities considered, the pdf results indicated that local extinction was occurring in the flame. Comparison with the experimental data is inconclusive, due to the level of scatter. However it is believed [19] that little, if any local extinction should be observed. A similar bimodal result was obtained by Chen et al. [20], who attributed the local extinction to the neglect of differential diffusion in the pdf calculations. However it should be observed that local extinction is only

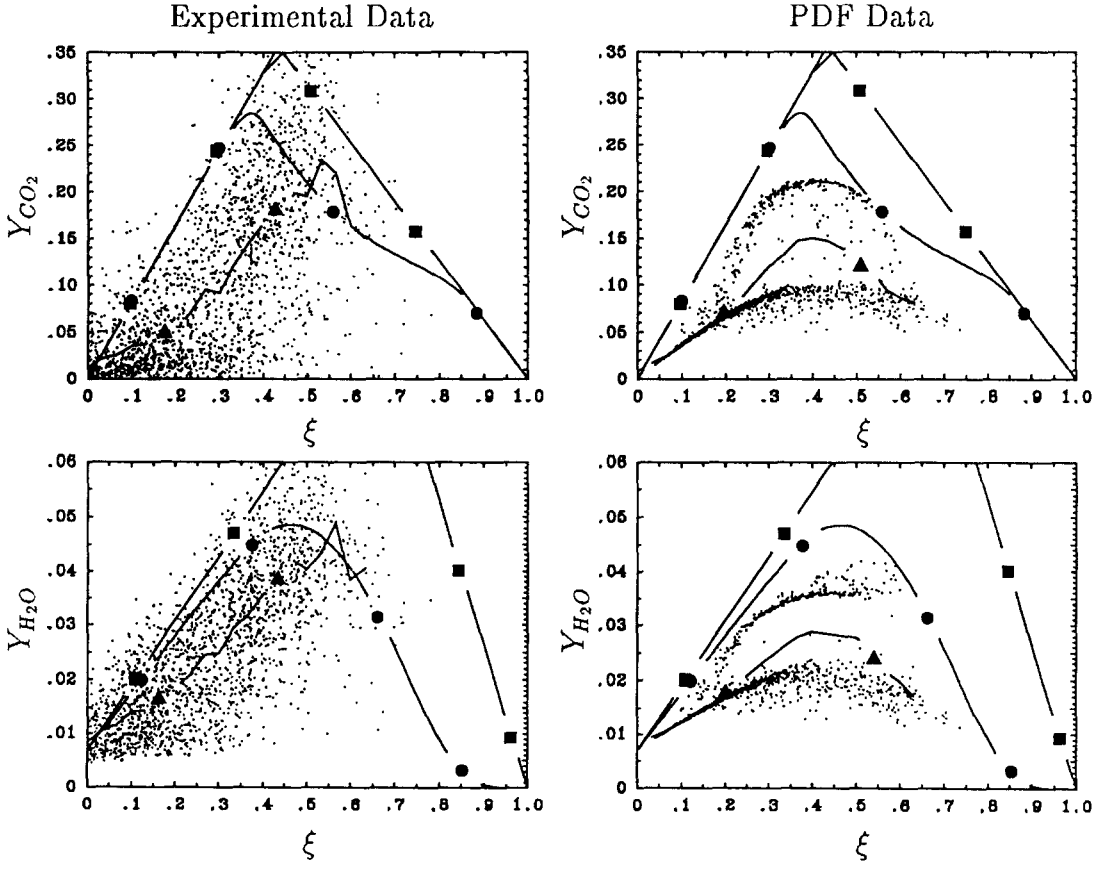

Fig. 5. Composition scatter plots for $CO/H_2/N_2$–air flame with jet velocity of 155 m/s. Experimental data in left column, pdf results in right column. –∅–, equilibrium values; –□–, border of allowed regions; –△–, conditional mean of data.

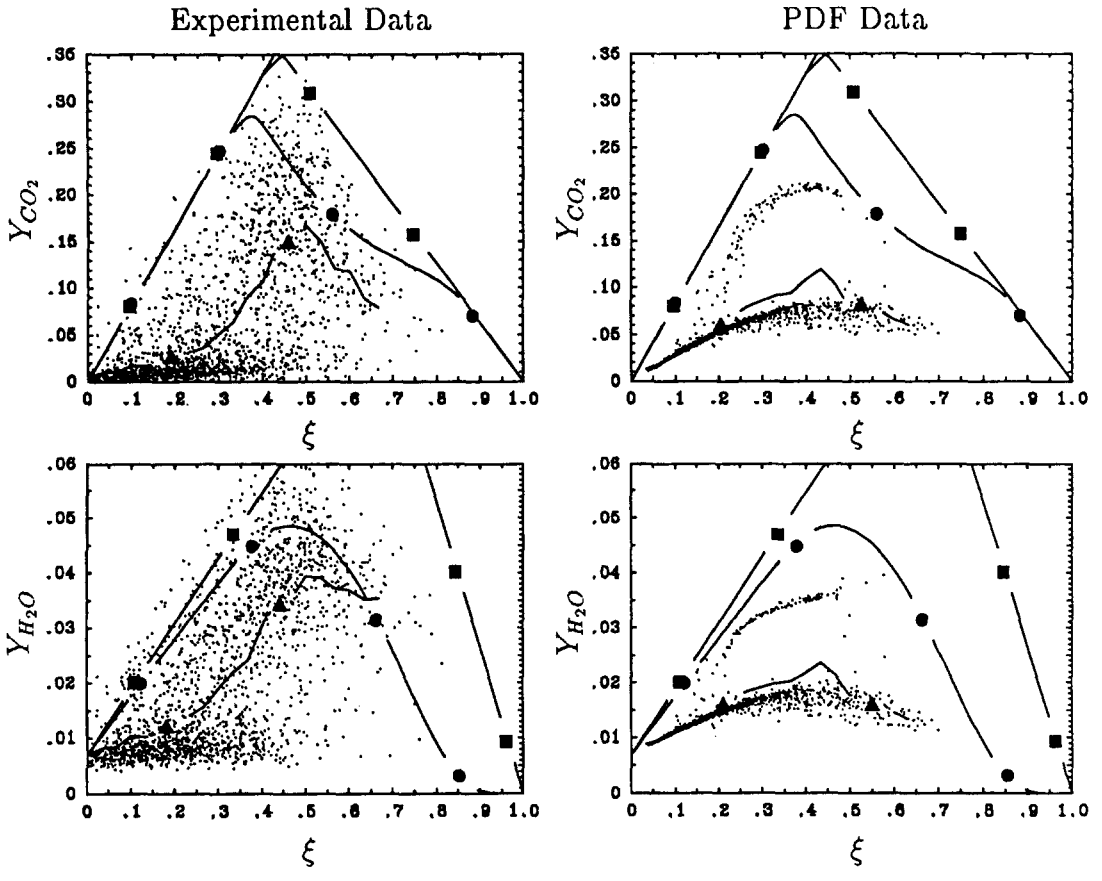

Fig. 6. Composition scatter plots for $CO/H_2/N_2$–air flame with jet velocity of 164 m/s. Experimental data in left column, pdf results in right column. –∅–, equilibrium values; –□–, border of allowed regions; –△–, conditional mean of data.

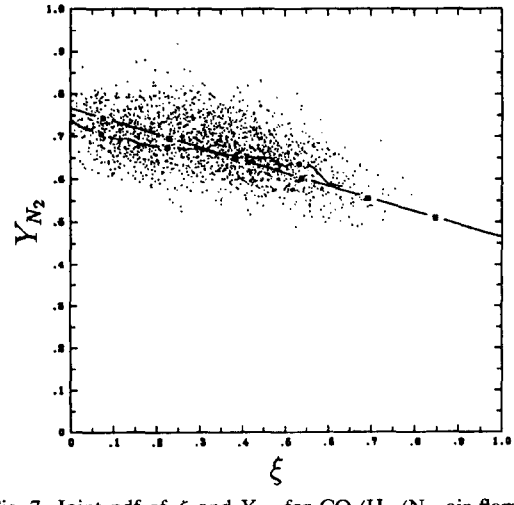

Fig. 7. Joint pdf of ξ and Y_{N_2} for $CO/H_2/N_2$–air flame with jet velocity of 98 m/s. Points are experimental data. –∅–, conditional mean $\langle Y_{N_2}|\xi\rangle$; –□–, joint pdf for the case of equally diffusive species and inert N_2.

predicted for flames with jet velocities within 10% of the extinction velocity.

Complete extinction for the flame was found to occur experimentally at a jet velocity of 167.0 m/s. For the pdf calculations, a bulk jet velocity of 175.0 m/s was found to show almost no trace of reacting particles, indicating that extinction was being predicted within 5% of the experimental value.

CONCLUSION

The velocity-dissipation-composition pdf method has been used to model a $CO/H_2/N_2$–air-piloted turbulent diffusion flame in the regime of extinction. A feature of the solution method was the modeling of the reaction by a reduced mechanism obtained by the ILDM method. The pdf model was found to produce scatter plots of composition that were quantitatively similar to the experimental

data, with extinction occurring at approximately the same jet velocity as the experiment.

A small amount of local extinction was predicted by the pdf method for flames with a jet velocity within 10% of the extinction velocity, while experimental evidence indicates that there should be none. It is thought that the cause of this local extinction prediction is the neglect of differential diffusion in the pdf calculations. However, the degree of scatter in the experimental data does not rule out the presence of a small amount of local extinction occurring.

These result has demonstrated that the solution of pdf transport equation for large-dimensional problems is tractable for relatively complex flows, and capable of yielding accurate results. Also it has shown that reduced mechanisms produced by the ILDM method can be used in turbulent 'real life' flows, and with good results.

The authors would like to thank A. Masri for the use of his experimental data, and U. Maas for the ILDM-reduced mechanism used in the pdf calculations. This work was supported in part by the National Science Foundation Grant CBT-8814655 and in part by the U.S. Air Force Office of Scientific Research (Grant No. F49620-94-1-0098). Computations conducted during the research were performed on the Cornell National Supercomputer Facility, which is supported in part by the National Science Foundation, New York State, The IBM Corporation, and members of the Corporate Research Institute.

REFERENCES

1. Pope, S. B., *Prog. Ener. Combust. Sci.* 11:119–192 (1985).
2. Pope, S. B., *Twenty-Third Symposium (International) on Combustion*, The Combustion Institute, Pittsburgh, 1990, pp. 591–611.
3. Masri, A. R., Dibble, R. W., and Barlow, R. S., *Combust. Flame*, in press.
4. Maas, U. A., and Pope, S. B., *Combust. Flame* 88:239–264 (1992).
5. Maas, U. A., and Pope, S. B., *Twenty-Fourth Symposium (International) on Combustion*, The Combustion Institute, Pittsburgh, 1992, pp. 103–112.
6. Pope, S. B., *Phys. Fluids A* 3:1947–1957 (1992). (Correction in 4:1008.)
7. Yeung, P. K., and Pope, S. B., *J. Fluid Mech.* 207:531–586 (1989).
8. Norris, A. T., Ph.D. thesis, Cornell University, 1993.
9. Anand, M. S., Pope, S. B., and Mongia, H. C., AIAA 31st Aerospace Sciences Meeting and Exhibit, Reno, Nevada, pages AIAA-93-0106, 1992.
10. Dopazo, C., *Phys. Fluids* 18:397–404 (1975).
11. Eswaran, V., and Pope, S. B., *Phys. Fluids* 31:506–520 (1988).
12. Curl, R. L., *A. I. Ch. E. J.* 9:175–181 (1963).
13. Norris, A. T., and Pope, S. B., *Combust. Flame* 83:27–42 (1991).
14. Nguyen, T. V., and Pope, S. B., *Combust. Sci. Technol.* 42:13–45 (1984).
15. Chen, J. Y., and Kollman, W., *Seventh International Symposium on Turbulent Shear Flows*, 1989, pp. 126–148.
16. Maas, U., and Pope, S. B., *Twenty-Fifth Symposium (International) on Combustion*, The Combustion Institute, Pittsburgh, in press.
17. Pope, S. B., and Gadh, R., *Commun. Statist. Simul.*, 17:349–376 (1988).
18. Hinze, J. O., *Turbulence*, 2nd ed., McGraw-Hill, New York, 1975.
19. Masri, A. R., and Dibble, R. W., *Twenty-Second Symposium (International) on Combustion*, The Combustion Institute, Pittsburgh, 1988, pp. 607–618.
20. Chen, J. Y., Dibble, R. W., and Bilger, R. W., *Twenty-Third Symposium (International) on Combustion*, The Combustion Institute, Pittsburgh, 1990, pp. 775–780.

Received 1 December 1993; revised 20 April 1994

Comments

M. A. Delichatsios, Factory Mutual Research, USA. In your mixing model, you have assumed that the effective strain rate is ε/k; this way, Kolmogorov scale effects have been ignored. Can you comment on the validity of ignoring Kolmogorov time scale effects? Or why is the large scale straining rate, rate controlling?

Authors' Reply. For the flow conditions studied we assume that the Reynolds number is large enough so that the dissipative process is controlled by the large scales of turbulence, and hence is independent of the diffusivity. However, this also requires the assumption that the reaction rate is independent of molecular dif-

fusion; we have distributed combustion rather than a flamelet-like process. These assumptions can be justified by the following observations: The jet Reynolds number is of order 50,000; the fuel-air mixture has a very broad reaction zone (compared to hydrocarbon fuels); the flow is close to extinction.

R. W. Bilger, University of Sydney, Australia. It is clear that the chemical reaction rate terms are closed in the partial differential equations for the joint probability density function. It is not clear, however, that they remain so in the Monte Carlo simulation of these equations in which stochastic particles mix in sudden events followed by periods of chemical reaction. In the real world reaction and diffusion occur simultaneously and in the reaction zones of flame they lead to a delicate balance for the radicals and other intermediates such as H, which are all important in determining reaction rates. Can you show that your mixing and chemistry models reproduce the correct physics of what actually happens in a flame?

Authors' Reply. In order to minimize the effect of discrete mixing and reaction processes, we chose a continuous mixing model so there would be no sudden jumps in the particle compositions. The errors associated with performing the mixing and reaction in two separate steps were also addressed by a two-step checking process, to ensure the order in which the two processes were performed did not bias the solution. So from a numerical point of view, we have attempted to perform the reaction and mixing in as near to a simultaneous process as possible.

On a more fundamental level, the reduced mechanism was obtained without considering that the fast-reacting intermediate species levels may be affected by the small-scale diffusion process. Whether the flow contains flamelet-like structures for the fast-reacting intermediates, embedded in the distributed combustion field of the slow-reacting major species and what effect this may have on the resulting reduced mechanism has not been studied.

J. Chomiak, Chalmers University of Technology, Sweden. Your mixing model excludes flamelets. Do you consider the very specific molecular mixing and reaction mechanism of the strained flamelets to be negligible and how would you define the limitation of your approach?

Authors' Reply. As mentioned in reply to the question of M. A. Delichatsios, the flow modeled in this study is far from the flamelet regime and so we consider the effect of the small scale diffusion process to be negligible for this flow. However, for flows where the flamelet description is applicable, the current mixing model would be deficient. This can be remedied by including information about the scalar gradient into the joint pdf transport equation. This would allow the small scale diffusion process to be accounted for and so extend the applicability of the PDF method into the flamelet regime.